ANALYSIS OF PROPAGATION CHARACTERISTICS OF HYDROGEN FLAME IN SHOCK TUBE IN INTEGRATED ENERGY SYSTEM

by

Baohua ZHAO *

School of Chemistry and Chemical Engineering,
Nanjing University of Science and Technology, Nanjing, Jiangsu, China

Original scientific paper
https://doi.org/10.2298/TSCI2302059Z

In order to study the explosion law of hydrogen and air premixed gas in the pipeline, the author proposes an analysis of the propagation characteristics of hydrogen in the shock tube in the integrated energy system. Use a square transparent pipe with a size of 150 mm×150 mm×1000 mm, the shape of the explosion flame, the propagation velocity and the pressure change with the hydrogen volume fraction from 10-40% were observed through experiments. Flame spread and pressure were recorded and measured by high speed cameras and pressure sensors, respectively. Experimental results show that the explosion flame characteristics and pressure changes are greatly affected by the hydrogen volume fraction. With the increase of hydrogen volume fraction, the maximum velocity and maximum value of flame in pipe increase significantly. The maximum flame propagation speed is increased from 18.3-304.2 m/s, and the propagation time is shortened from 123.5-10.5 ms. The pressure peak increased from 2.95-34.06 kPa. The analysis of the propagating characteristics of the hydrogen flame in the shock tube in the integrated energy system can well reflect the intensity of the hydrogen explosion. Do not use abbreviations and acronyms in the abstract.

Key words: *pipe-line, hydrogen explosion, flame velocity, flame structure, flow field characteristics, integrated energy system*

Introduction

With the continuous development of technology, the level of energy consumption is also continuously increasing, and energy development is gradually changing from growth to quality and development [1, 2]. An energy transition is essential and urgent to prevent an aging economy. A hybrid energy system refers to an energy system that can accept multiple energy sources, use smart devices to determine user needs, and store energy sources in a proposed plan consisting of an energy supply network, energy exchange, and energy storage unit, terminal integrated power supply unit and end users, in practical use it appears as distributed power supply system and regional power system [3].

The CO includes substances such as hydrogen, CO, CH_4, ethane, propane, ethylene, *etc.*, while hydrogen has special properties and is currently the cleanest fuel and is increasingly used [4]. Hydrogen is an important industrial material and the most important fuel and special fuel, but compared to conventional fuels and flammable gases due to its low electrical energy, wide explosion, laminar burning speed and high diffusion speed due to its explosive power and greater damage, the incidence of hydrogen explosions has increased in recent years [5]. At pres-

* Author's e-mail: zhaobaohua7@163.com

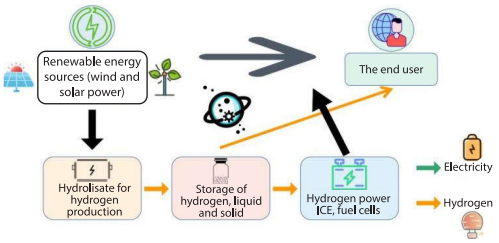

Figure 1. Propagation of hydrogen flame in shock tube in integrated energy system

ent, most scientists are focusing on the study of the explosive properties of hydrogen, but the hydrogen explosion is easily changed by the environment, especially the spatial scale [6]. A large eddy simulation (LES) model performed a numerical simulation of the effect of the mass ratio on the surface of the hydrogen-air explosion process, with special attention the analysis of the effect of the effect on the flame velocity, the relationship between turbulence and the transition of the fire front, *etc.* As shown in fig. 1.

Literature review

Kamlesh *et al*. [7] tested hydrogen and methane in closed tubes and found that hydrogen is explosive and can cause serious damage. Singh *et al*. [8] and Sra *et al*. [9] first discovered that the reason hydrogen is more harmful than methane and ethane is due to the fact that hydrogen itself is highly flammable.

There are many studies on gas explosions at home and abroad, but there are some studies on hydrogen explosions, especially the characteristics of flame content and post-explosion pressure need further investigation. The author conducted experiments in a small horizontal square tube with a length of 1 m and found that the properties of diffusion, diffusion velocity, and explosion pressure change the characteristics of the explosion flame of a hydrogen-air mixture with different volumes of hydrogen.

Methods

Integrated energy system

There are two strategies to deal with the energy crisis, namely *open source* and *throttling*. *Throttling* focuses on reducing additional losses on the energy consumption side and improving energy efficiency, it is very important in both single energy system and integrated energy system [10-16]. *Open source* refers to reducing the use of traditional energy sources, actively develop and utilize clean energy, such as wind energy, tidal energy, and solar energy. However, the intermittency and randomness of renewable energy lead to its lack of stability in transmission, distribution and use, resulting in low energy utilization efficiency and difficulty in ensuring energy reliability. Some experts pointed out: the Energy Internet, consisting of renewable energy, power systems and information and communication technologies, will be the core of the third industrial revolution, the integrated energy system is the foothold of the energy Internet and smart energy, which involves energy conversion. The integrated energy system is based on the theory of multi-energy complementation and energy cascade utilization, which can vigorously develop renewable resources, effectively control energy consumption, further improve energy utilization efficiency, it is of great significance to cope with severe challenges such as the surge in energy demand, environmental pollution, and climate change.

Test device

The test device mainly includes transparent square plexiglass pipes (dimensions are 150 mm × 150 mm × 1000 mm, effective volume 22.5 L). The gas distribution system mainly includes high pressure hydrogen cylinder (the purity of hydrogen is 99.999%), GTL air generator, Alicat-M mass-flowmeter, *etc.* The ignition system consists of high frequency pulse ignit-

er, 6V DC power supply and switch. The high speed camera system consists of Lavision-VC high speed camera, controller and computer. The data acquisition system includes MD-HF type pressure sensor, E12S type photoelectric sensor, MCC-1608FS type data acquisition card and computer.

Numerical model

In the large eddy simulation, the N-S equation is filtered by introducing a filter function, so that the waves with high wave numbers are truncated, but the energy transfer process remains, that is, it is allowed to transfer from the large eddy to the small eddy. The control equation of LES:

$$\frac{\partial \overline{\rho}}{\partial t}+\frac{\partial\left(\overline{\rho}\tilde{u}_i\right)}{\partial x_i}=0 \tag{1}$$

$$\frac{\partial\left(\overline{\rho}\tilde{u}_i\right)}{\partial t}+\frac{\partial\left(\overline{\rho}u_i\tilde{u}_j+\overline{p}\delta_{ij}-\tilde{\tau}_{ij}+\tau_{ij}^{\mathrm{sgs}}\right)}{\partial x_j}=0 \tag{2}$$

$$\rho\frac{\mathrm{d}^2x}{\mathrm{d}t^2}=\frac{\partial\sigma_x}{\partial x} \tag{3}$$

where the parameters of LES filtering are marked as horizontal lines, and the parameters of quality weight filtering are marked with wavy lines. The ρ [kgm^{-2}] is the density, p [Pa] – the pressure, u_i and u_j are the velocity components, t [second] – the time, σ_{ij} [Nsm^{-2}] – the stress tensor determined by the molecular viscosity, which can be expressed as

$$\sigma_{ij}=\mu\left(\frac{\partial u_i}{\partial x_j}+\frac{\partial u_j}{\partial x_i}\right)-\frac{2}{3}\mu\frac{\partial u_k}{\partial x_k}\delta_{ij}$$

τ_{ij} [Nm^{-3}] – the sub-grid scale stress, define it as

$$\tau_{ij}=\rho\widetilde{\tilde{u}_i\tilde{u}_j}-\rho\tilde{u}_i\tilde{u}_j$$

h_s [Jkg^{-1}] – the apparent enthalpy and λ [Wm^{-1}K^{-1}] – the thermal conductivity. The subgrid enthalpy flux can be approximated by the gradient assumption as:

$$\rho\left(\widetilde{u_ih_s}-\tilde{u}\tilde{h}_s\right)=-\frac{\mu_{\mathrm{SGS}}c_p}{\mathrm{Pr}_{\mathrm{SGS}}}\frac{\partial T}{\partial x_j}$$

among them, μ_{SGS} [Nsm^{-2}] – the subgrid viscosity, $\mathrm{Pr}_{\mathrm{SCS}}$ – the subgrid Prandtl number, c_p [Jkg^{-1}K^{-1}] – is the constant pressure specific heat, and T [°C] – the temperature.

For premixed combustion, the author adopts the Zimont combustion flame surface sublattice model based on the C equation, where c is the reaction progress variable, in the simulation process, it is taken as the $c = 0.1$ flame front, and the filtered expression of the C equation:

$$\frac{\partial}{\partial t}\left(\overline{\rho}\tilde{c}\right)+\frac{\partial}{\partial x_j}\left(\overline{\rho u_j}\tilde{c}\right)=\frac{\partial}{\partial t_j}\left(-\frac{\mu+\mu_t}{Sc_t}\frac{\partial\tilde{c}}{\partial x_j}\right)+S_{\mathrm{c}} \tag{4}$$

where u_j (j = 1, 2, 3) is the velocity in the x-, y-, and z-directions and S_c – the process variable source term

$$c = \frac{\sum_{i=1}^{n} Y_i}{\sum_{i=1}^{n} Y_{i,\mathrm{eq}}} \tag{5}$$

where n is the number of combustion products, species, Y_i – the mass fraction of product component i, $Y_{i,\mathrm{eq}}$ – the mass fraction of equilibrium product component i. According to the definition of eq. (5), $c = 0$ in the final combustion mixture, $c = 1$ in the combustion product, $0 < c < 1$at the flame surface, $\overline{S}_c$ – the source term of the process variable:

$$\overline{S}_{\mathrm{c}} = A\left(u'\right)^{3/4} \rho_{\mathrm{u}} U_1^{\,1/2} \alpha^{-1/4} \left|\nabla \tilde{c}\right| l_{\mathrm{t}}^{1/4} \tag{6}$$

where the model constant $A = 0.52$, u [ms^{-1}] – the sublattice turbulent pulsation velocity, ρ_u [kgm^{-3}] – the density of the final combustion mixture, U_1 [ms^{-1}] – the laminar combustion velocity, α – the heat transfer coefficient of reactant molecules, and l_t – the characteristic scale of turbulent flow.

Test method and repeatability

Test method

The test pipe-line is placed horizontally, and the inflation port, igniter, and pressure sensor are installed at the right end of the pipe-line, the igniter is located in the center of the right end, and the photoelectric sensor is located above the pipe at the right end, facing the igniter, in order to mark the starting moment of ignition. The basic steps of the test process are: install film, distribute gas, ignite, collect pressure and photoelectric signals, and collect flame pictures. The hydrogen volume fractions in the hydrogen-air premix used in this experiment were 10%, 15%, 20%, 25%, 30%, and 40%, respectively.

The gas distribution method is the air exhaust method, that is, when the right end of the pipe-line is filled with hydrogen/air premixed gas, the air is exhausted above the left end. Collection of pressure and photoelectric signals and flame pictures: the collection frequency of pressure and photoelectric signals is 15 kHz. The shooting of the flame propagation process was carried out in a dark environment to ensure a clear flame, and the high speed camera was used for high speed shooting at 2000 fps, in order to capture the explosion flame structure and the position of the flame front.

Test repeatability

In this paper, the experimental test of the preliminary mixture of 40% of the 20% of the 20% of the different hydrogen in the different hydrogen volume was tested, and the repeated test of the gas fraction of the different hydrogen volume scores was conducted more than three times, to ensure the reliability of the result. The difference between the velocity and pressure of flame propagation in the deceleration process is analyzed. The results show that the method is small and repeatable [17].

Results and discussion

Characteristics of hydrogen explosion flame propagation

The flame process captured by high speed camera is accurate, and the color of flame, source and shape of the front flame can be seen. Because the color of premixed explosive flame is light when hydrogen volume fraction is 10%, high speed camera cannot detect pure flame

retardant process. A simple screenshot of the hydrogen-air premixed gas explosion flames with hydrogen volume fractions of 15%, 20%, 25%, 30%, and 40% was taken in chronological order.

The hydrogen explosion rate in the pipe-line increases with the increase of hydrogen volume fraction. When the hydrogen volume fraction is 10, the explosion can be heard. When the volume fraction is 20%, the explosion noise is suppressed and the laboratory has strong vibration. When the volume fraction of hydrogen was 25%, 30%, and 40%, the hydrogen cracking rate was achieved outdoors, and the noise was higher.

Propagation speed of hydrogen explosion flame

When studying the propagation of flame crack, image processing technology is used to calculate the propagation of flame crack. The calculation of flame propagation speed is simple and accurate. First, the position of the foreflame is calculated. The velocity field is the ratio of the different positions to the different times between the two positions. Using this method, the flame propagation characteristics of different hydrogen sources at different time points were calculated, and the flame propagation characteristics were obtained as shown in figs. 2 and 3. Due to the limitation of the length and emission of the pipe, the calculated flame velocity is mainly the flame velocity in the pipe, and the flame discharge condition of the nozzle is not studied. The time corresponding to the last data point of each curve in figs. 2 and 3 is the time when the flame reaches the nozzle [18].

It can be seen from figs. 2 and 3 that the velocity distribution and structure of the flame retardant are different in different hydrogen storage conditions. When the volume fraction of hydrogen is 15% and 20%, the flame propagation speed first increases, but with the appearance of irregular front and *tulip flame*, the flame propagation speed increases; When the hydrogen volume fraction is 25%, 30%, and 40%, the flame retardance of the pipe does not decrease, that is, it also increases [19].

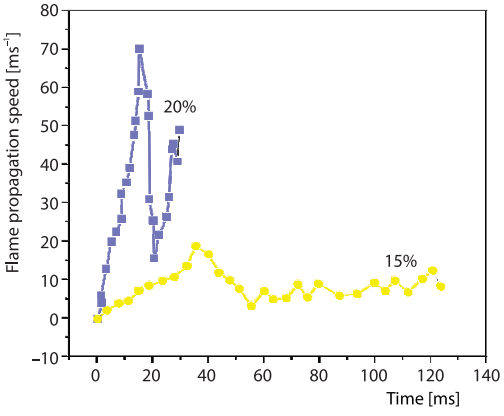

Figure 2. The flame propagation velocity when the hydrogen volume fraction is 15% and 20%

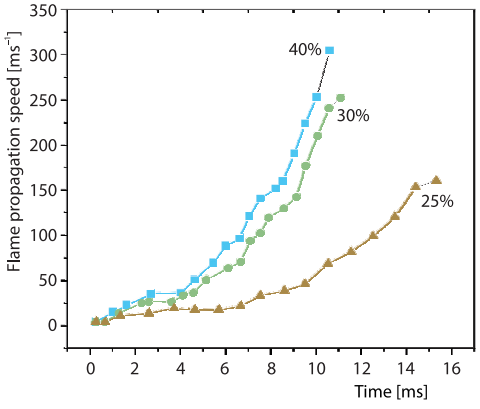

Figure 3. The flame propagation speed when the hydrogen volume fraction is 25%, 30%, and 40%

After calculation, it is concluded that when the hydrogen volume fraction is 15%, 20%, 25%, 30%, and 40%, the time it takes for the flame to reach the nozzle is 123.5 ms, 31.0 ms, 15.5 ms, 11.0 ms, and 10.5 ms, respectively, the corresponding average flame propagation velocities are 8.1 m/s, 32.3 m/s, 64.5 m/s, 90.9 m/s, and 95.2 m/s, respectively, the corresponding maximum flame propagation speeds are 18.3 m/s, 59.6 m/s, 159.6 m/s, 254.2 m/s,

304.2 m/s, respectively, the time points at which the maximum flame propagation velocity appeared were 36.0 ms, 17.5 ms, 15.5 ms, 11.0 ms, and 10.5 ms, respectively. It can be seen that the flame propagation is greatly affected by the volume fraction of hydrogen. As the hydrogen volume fraction increases, the maximum and average velocity of the flame in the tube doubles. The maximum speed increased from 18.3 m/s to 304.2 m/s and the average speed increased from 8.1 m/s to 95.2 m/s.

Variation characteristics of hydrogen explosion pressure

The measurement precision depends on the fire end of the pipe-line, 20 mm away from the ignition point. The change of crack overpressure in different hydrogen volume fraction is recorded by pressure sensor, as shown in figs. 4 and 5. It can be seen from figs. 4 and 5 that when hydrogen volume fractions are 10% and 15%, the pressure wave [20] has weak oscillation.

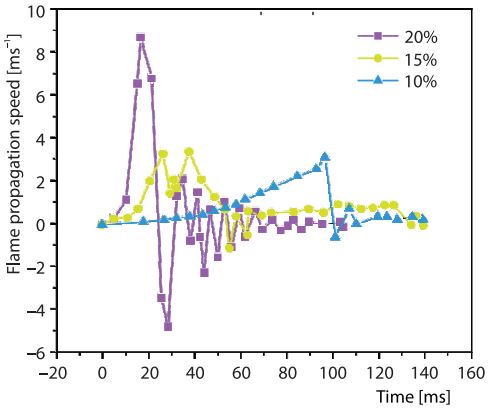

Figure 4. Variation of explosion pressure with hydrogen volume fraction of 10%, 15%, and 20%

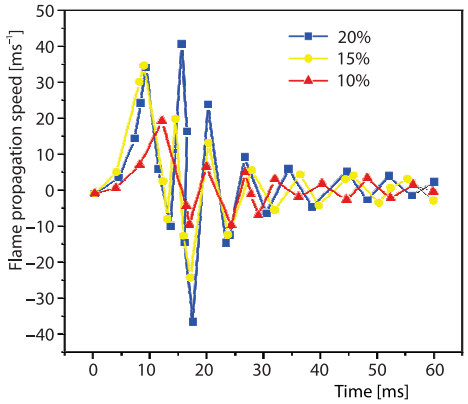

Figure 5. Variation of explosion pressure with hydrogen volume fraction of 25%, 30%, and 40%

That with the increase of hydrogen volume fraction, the initial peak value of explosion pressure increases rapidly, and the time required to reach the maximum value decreases. The explosion flame propagation at each volume fraction is compared with the corresponding time of the pressure peak, as shown in tab. 1.

Combining the data in tab. 1, figs. 4 and 5, it can be concluded that the pressure first reaches the peak value, and then the flame is transmitted to the nozzle, and after a period of time, the pressure returns to the initial value. As the hydrogen volume fraction increases, the smaller the time difference between the peak pressure and the time it takes for the flame to reach the nozzle, the longer it takes for the pressure to return to the initial value.

Table 1. Corresponding time of explosion flame propagation and pressure peak

Hydrogen volume fraction [%]	10	15	20	25	30	40
First pressure peak [kPa]	2.95	3.75	8.68	20.00	33.75	34.06
The moment of the first pressure peak [ms]	97.0	26.0	18.0	11.8	9.0	9.5
The moment when the maximum flame propagation speed occurs [ms]	–	36.0	17.5	15.5	11.0	10.5
The time it takes for the flame to reach the nozzle [ms]	–	123.5	31.0	15.5	11.0	10.5

Note: – in the table indicates lack of data.

When the hydrogen volume fraction is high (20%, 25%, 30%, and 40%), after the pressure wave reaches the peak, there will be several strong oscillations (the first negative pressure value generated by the two oscillations with the largest amplitude, the secondary peak value and the second negative pressure value are shown in tab. 2) and multiple small oscillations. The reason for this phenomenon is: from the start of ignition, the reaction continues to accumulate pressure, the pipe after the film is ruptured is a semi-closed space, and part of the combustible gas in the pipe is flushed out, at the same time, the reaction is still going on, and the gas in the pipe-line participates in the reaction, which causes the pressure in the tube to drop, resulting in negative pressure.

Table 2. The positive and negative peaks of explosion pressure oscillation when the hydrogen volume fraction is high

Hydrogen volume fraction [%]	20	25	30	40
First pressure peak [kPa]	8.68	20.00	333.75	34.06
The first negative pressure value [kPa]	–4.64	–9.48	9.34	–10.52
Secondary peak [kPa]	2.21	7.72	21.86	41.01
The second negative pressure value [kPa]	–1.04	–11.09	–26.48	–38.17

Conclusion

The propagation characteristics of hydrogen in the shock tube of the combined turbine are analyzed. The flame characteristics, velocity distribution and pressure change characteristics of premixed gas explosion under different hydrogen volume fraction were analyzed experimentally. The results show that the three factors are greatly affected by the volume fraction of hydrogen in premixed fuel. The maximum velocity of the flame and the peak explosion pressure increase with the increase of the volume fraction of hydrogen, which results in a great influence on the hydrogen explosion intensity.

References

[1] Yaseen, S., *et al.*, *In-situ* Species,P hotocorrosion Inhibition of Sulphide-Based Nanomaterials for Energy Production through Photocatalytic Water splitting, *International Journal of Energy Research, 46* (2022), 2, pp. 634-666
[2] korss. An Improved Method for Estimating the Veocity Fieeld of Corona1 Propagating Disturbances, *Solar Physics, 297* (2022), 8, pp. 1-15
[3] Li, L., *et al.*, *In-situ* Species, An Integrated Solution Minimize the Energy Consumption of a Resource-Constrained Machining System, *IEEE Transactions on Automation Science and Engineering, 17* (2020), 3, pp. 1158-1175
[4] Aminov, R. Z., Application of Multifunctional Systems with Latent Heat Thermal Energy Storages: A Way to Improve NPP Safety and Efficiency, *Thermal Engineering, 69* (2022), 8, pp. 555-562
[5] Jiang, Q., *et al.*, *In-situ* Species, Simultaneous Removal of Hydrogen Sulfide and Ammonia in the Gas Phase: A Review, *Environmental Chemistry Letters, 20* (2022), 2, pp. 1403-1419
[6] Guney, M., *et al.*, *In-situ* Species, Contamination by As, Hg, and Sb in a Region with Geogenic as Anomaly and Subsequent Human Health Risk Characterization, *Environmental Monitoring and Assessment*, *192* (2020), 1, pp. 1-16
[7] Kamlesh., *et al.*, *In-situ* Species, Influence of the Channel Profile on the Thermal Resistance of Closed-loop Flat-Plate Oscillating Heat Pipe, *Journal of the Brazilian Society of Mechanical Sciences and Engineering, 42* (2020), 3, pp. 1-12
[8] Singh, A., *et al.*, *In-situ* Species, Control implementation of squirrel cage induction generator based wind Energy Conversion System, *Journal of scientific and industrial research, 79* (2020), 4, pp. 306-311

[9] Sra, B., *et al.*, *In-situ* Species, Experimental Study of end-Vented Hydrogen Deflagrations in a 40-Foot Container, *International Journal of Hydrogen Energy, 45* (2020), 31, pp. 15710-15719
[10] Chen, B., *et al.*, *In-situ* Species, Numerical Simulation of the Influence of Vent Conditions on the Characteristics of Hydrogen Explosion in Confined Space, *Combustion Theory and Modelling, 26* (2022), 2, pp. 241-259
[11] Naumenko, V. V., *et al.*, *In-situ* Species, Study of Reasons for the Blistering Formation on Metal Surface after the Tests on Hydrogen Induced Cracking and Classification of Blisterings, *Steel in Translation, 52* (2022), 2, pp. 263-269
[12] Smygalina, A. E., *et al.*, *In-situ* Species, On the Efficiency of Utilization of Hydrogen and Syngas in a Spark-Ignition Engine, *Journal of Engineering Physics and Thermophysics, 95* (2022), 1, pp. 168-176
[13] Buyukakn, M. K., *et al.*, *In-situ* Species, Numerical Investigation on Hydrogen-Enriched Methane Combustion in a Domestic Back-Pressure Boiler and Non-Premixed Burner System from Flame Structure and Pollutants Aspect, *International Journal of Hydrogen Energy, 45* (2020), 60, pp. 35246-35256
[14] Pearroya, P., *et al.*, *In-situ* Species, Orbit Propagation Around Small Bodies Using Spherical Harmonic Coefficients Obtained from Polyhedron Shape Models, *Proceedings of the International Astronomical Union, 15* (2021), S364, pp. 203-210
[15] Yu, C., *et al.*, *In-situ* Species,Reaction-Diffusion Manifolds Including Differential Diffusion Applied to Methane/Air Combustion in Strong Extinction Regimes, *Combustion Theory and Modelling*, *26* (2022), 3, pp. 451-481
[16] Zhang, Q., Relay Vibration Protection Simulation Experimental Platform Based on Signal Reconstruction of MATLAB Software, *Non-linear Engineering, 10* (2021), 1, pp. 461-468
[17] Zheng, L., *et al.*, *In-situ* Species, Study on Explosion Characteristics of Premixed Hydrogen/Biogas/Air Mixture in a Duct, *International journal of hydrogen energy, 44* (2019), 49, pp. 27159-27173
[18] Peng, Y. H., *et al.*, *In-situ* Species, Principle and Structure of a Multi-Chamber Piezoelectric Pump with Large Flow Rate Integrated into Printed Circuit Board, *Journal of Intelligent Material Systems and Structures, 33* (2022), 15, pp. 1960-1974
[19] Lu, X., *et al.*, *In-situ* Species, Experimental and Kinetic Study of Laminar Flame Characteristics of H_2/O_2/Diluent Flame under Elevated Pressure, *International Journal of Hydrogen Energy, 45* (2020), 56, pp. 32508-32520
[20] Wu, Z., *et al.*, *In-situ* Species, Investigation of Flame Characteristics of Hydrogen Jet Issuing into a Hot Vitiated Nitrogen/Argon/Carbon Dioxide Coflow, *International Journal of Hydrogen Energy, 44* (2019), 52, pp. 28357-28370

Paper submitted: June 29, 2022
Paper revised: August 23, 2022
Paper accepted: August 31, 2022